

Adenomatous Polyposis Coli on Microtubule Plus Ends in Cell Extensions Can Promote Microtubule Net Growth with or without EB1

Katsuhiko Kita,* Torsten Wittmann,*† Inke S. Näthke,‡ and
Clare M. Waterman-Storer*

*Department of Cell Biology, The Scripps Research Institute, La Jolla, CA 92037; and †Division of Cell and Developmental Biology, School of Life Sciences, University of Dundee, Dundee DD1 5EH, United Kingdom

Submitted June 7, 2005; Revised January 31, 2006; Accepted February 24, 2006
Monitoring Editor: Ted Salmon

In interphase cells, the adenomatous polyposis coli (APC) protein accumulates on a small subset of microtubules (MTs) in cell protrusions, suggesting that APC may regulate the dynamics of these MTs. We comicroinjected a nonperturbing fluorescently labeled monoclonal antibody and labeled tubulin to simultaneously visualize dynamics of endogenous APC and MTs in living cells. MTs decorated with APC spent more time growing and had a decreased catastrophe frequency compared with non-APC-decorated MTs. Endogenous APC associated briefly with shortening MTs. To determine the relationship between APC and its binding partner EB1, we monitored EB1-green fluorescent protein and endogenous APC concomitantly in living cells. Only a small fraction of EB1 colocalized with APC at any one time. APC-deficient cells and EB1 small interfering RNA showed that EB1 and APC localized at MT ends independently. Depletion of EB1 did not change the growth-stabilizing effects of APC on MT plus ends. In addition, APC remained bound to MTs stabilized with low nocodazole, whereas EB1 did not. Thus, we demonstrate that the association of endogenous APC with MT ends correlates directly with their increased growth stability, that this can occur independently of its association with EB1, and that APC and EB1 can associate with MT plus ends by distinct mechanisms.

INTRODUCTION

The dynamic microtubule (MT) cytoskeleton is critical to cell functions requiring the establishment and maintenance of morphological asymmetries. This includes cell division, directed cell migration, the immune response, and neuronal development. Twenty years ago, Mitchison and Kirschner (1986) hypothesized that MTs may mediate the establishment of cellular asymmetry via spatial regulation of plus end MT assembly/disassembly dynamics, resulting in asymmetric stabilization of MTs in specific regions of cells. In support of this idea, a number of specialized MT subsets have been identified in cells. For example, in migrating vertebrate tissue culture cells, a subset of MT plus ends that grow slowly and with infrequent catastrophes into the advancing leading edge, termed pioneer MTs, have been identified (Wadsworth, 1999; Waterman-Storer, 2002; Wittmann *et al.*, 2003). Another subset of MTs that are resistant to cold- or nocodazole-induced depolymerization

and are marked by posttranslational modification (detyrosinated “Glu” MTs) radiate toward the leading edge of migrating cells (Gundersen *et al.*, 1984). However, the molecular mechanism for establishing and maintaining these regionally stabilized MTs is not well clarified, and it is unknown whether these subsets of MTs are required for establishment and/or maintenance of cellular asymmetries.

MT plus end assembly/disassembly dynamics can be regulated by a relatively recently characterized class of MT-associated proteins that are called plus end-binding proteins (+TIPs). These include CLIP-170, EB-1, CLASP, MCAK, dynein/dynactin, and the adenomatous polyposis coli protein (APC) (Mimori-Kiyosue and Tsukita, 2003; Akhmanova and Hoogenraad, 2005). These proteins associate at or very near (within ~1–2 μm) to growing MT plus ends in the cell. Most +TIPs characterized so far disappear when the plus ends switch to shortening (Carvalho *et al.*, 2003; Mimori-Kiyosue and Tsukita, 2003). Many +TIPs have been shown to interact with one another, suggesting they form a complex at growing MT plus ends. At MT ends, +TIPs may play a role in the regulation of different aspects of MT assembly/disassembly dynamics, with CLIP-170 (Komarova *et al.*, 2002) and CLASP (Mimori-Kiyosue *et al.*, 2005) promoting rescue, and EB1 promoting dynamic instability (Tirnauer *et al.*, 1999; Rogers *et al.*, 2002).

Two +TIPs, CLASPs and APC, are good candidates for local subcellular regulation of MT plus-end assembly/disassembly dynamics because these proteins localize to subsets of MTs in specific cell regions (Näthke *et al.*, 1996; Akhmanova *et al.*, 2001; Wittmann and Waterman-Storer, 2005). Recent studies have examined the spatial regulation of CLASP association with MT subsets and its effects on

This article was published online ahead of print in *MBC in Press* (<http://www.molbiolcell.org/cgi/doi/10.1091/mbc.E05-06-0498>) on March 8, 2006.

  The online version of this article contains supplemental material at *MBC Online* (<http://www.molbiolcell.org>).

† Present address: Department of Cell and Tissue Biology, University of California at San Francisco School of Dentistry, 513 Parnassus Ave., HSW-616, Box 0512, San Francisco, CA 94143-0512.

Address correspondence to: Clare M. Waterman-Storer (waterman@scripps.edu).

Abbreviations used: APC, adenomatous polyposis coli; MT, microtubule.

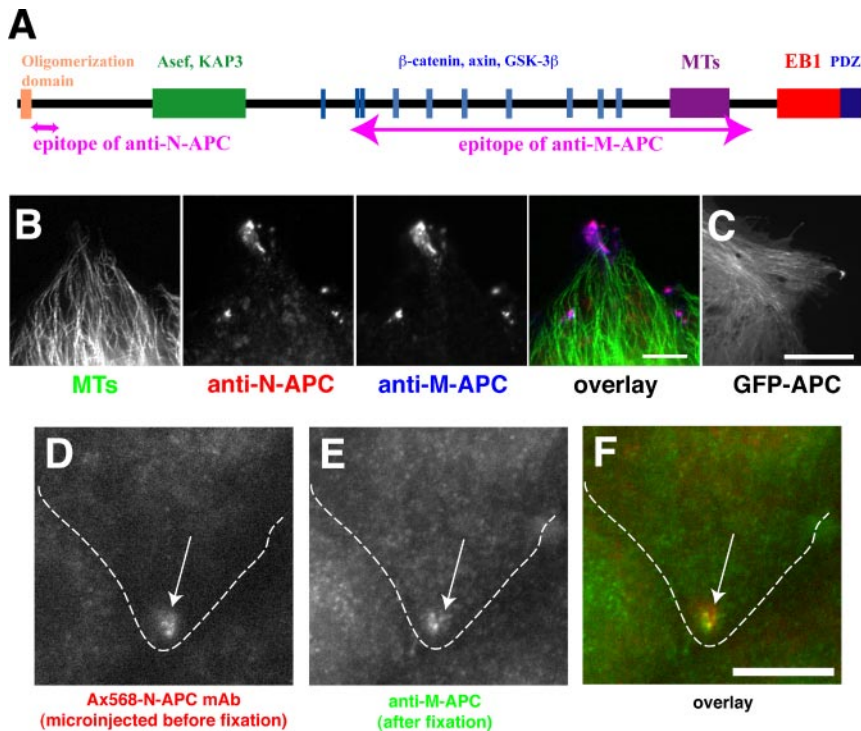


Figure 1. Alexa Fluor 568-labeled anti-N-APC mAb (Ax568-N-APC) as a probe to visualize endogenous APC. (A) Domain map of APC protein showing binding sites for specific proteins and epitopes of the antibodies used in this study. Note that the epitope of anti-N-APC is not overlapped with any known functional domains of APC. (B) Fixed MDCK cells were stained with anti-tubulin mAb (green; MTs), Ax568-N-APC (red; anti-N-APC), and anti-M-APC polyclonal antibody (blue; anti-M-APC). Both antibodies colocalize specifically to clusters near MT ends primarily in the cell protrusion. Bar, 5 μm . (C) GFP-APC expressed in MDCK cells, which, like endogenous APC localizes to clusters in the cell protrusion, also localizes along MT lattices throughout the cell. Also see Movie 1. Bar, 10 μm . (D–F) An MDCK cell was fixed 3 h after microinjection with Ax568-N-APC (outlined cell) and then followed by immunostaining. Ax568-N-APC (D), anti-M-APC (E), and merged image (F). Bar, 10 μm .

control of MT dynamic instability (Mimori-Kiyosue *et al.*, 2005; Wittmann and Waterman-Storer, 2005). Here, we focus on APC.

The subcellular distribution and dynamic behavior of APC in tissue cells is very unique (Näthke *et al.*, 1996; Dikovskaya *et al.*, 2001; Mimori-Kiyosue and Tsukita, 2001; Bienz, 2002). Immunofluorescence analysis of cultured cells has shown that APC accumulates in clusters on a few MT plus ends only near extended cell edges in interphase (Näthke *et al.*, 1996), whereas in mitosis it localizes to chromosomes at kinetochore–MT attachment sites (Fodde *et al.*, 2001; Kaplan *et al.*, 2001; Green and Kaplan, 2003). A small subset of green fluorescent protein (GFP)-tagged APC in living interphase cells has also been observed to move along MT lattices toward their plus ends in the periphery of cell extensions (Mimori-Kiyosue *et al.*, 2000a). There, APC accumulates in nonmembrane-bounded spherical clusters on growing MT ends. When these MTs switch from growth to shortening, APC clusters are reported to drop off MT ends and remain in the cell protrusion without MT association for several minutes before dissolving (Mimori-Kiyosue *et al.*, 2000a). Importantly, overexpression of APC makes MTs insensitive to depolymerizing drugs *in vivo* (Zumbrunn *et al.*, 2001), whereas purified APC promotes MT stability *in vitro* (Munemitsu *et al.*, 1994; Zumbrunn *et al.*, 2001). In addition, APC has been observed to localize to the tips of the subset of detyrosinated “Glu” MTs that are resistant to nocodazole-induced depolymerization (Wen *et al.*, 2004). Thus, APC on MT plus ends could contribute to the specific stabilization of MTs in interphase cell protrusions and in kinetochore fibers in the mitotic spindle.

APC encodes a 310-kDa multiple domain protein, identified as the gene responsible for familial adenomatous polyposis (Figure 1A) (Groden *et al.*, 1991; Joslyn *et al.*, 1991). Many proteins have been reported to interact with APC, and the interactive domains can be separated into three functionally distinct regions (Näthke, 2004). The N-terminal region contains

an oligomerization domain and an armadillo repeat that interacts with the MT motor kinesin II subunit KAP3 (Jimbo *et al.*, 2002); the Rac1-specific activator Asef (Kawasaki *et al.*, 2000); and IQGAP, an effector of Rac1 and Cdc42 (Watanabe *et al.*, 2004). The middle region is critical for the role of APC in Wnt signaling-mediated transcriptional regulation (Polakis, 2000). It contains short repeats that bind to the transcriptional activator β -catenin (Rubinfeld *et al.*, 1993; Su *et al.*, 1993), and it is essential for the regulation of β -catenin degradation (Munemitsu *et al.*, 1995). The C-terminal region of APC mediates the interaction of APC with MTs (Smith *et al.*, 1994). This occurs by a direct MT binding domain (Smith *et al.*, 1994; Zumbrunn *et al.*, 2001) or indirectly via an interaction with the +TIP protein EB1 (Su *et al.*, 1995). In addition, the C terminus of APC can bind to PDZ domain proteins, including human discs large (Matsumine *et al.*, 1996).

Because C-terminal truncations of APC found in familial and sporadic colorectal cancers lead to the loss of its direct association with MTs (Smith *et al.*, 1994), cytoskeletal regulation by APC may be important for the maintenance of normal intestinal epithelial function, including cell migration (Dikovskaya *et al.*, 2001; Näthke, 2004). How APC regulates MTs in cells, and whether this requires its interaction with other MT-associated proteins such as EB1 is not clear (Dikovskaya *et al.*, 2001). Previous studies have shown that overexpression of an APC construct with an intact EB1 binding domain but lacking the direct MT binding site still localized to MTs; however, it did not stabilize them against nocodazole treatment (Zumbrunn *et al.*, 2001). Although these data suggests that direct MT binding by overexpressed APC can promote MT stabilization, it does not provide information on how endogenous APC normally modulates the assembly/disassembly dynamics of MT plus ends in cells.

We set out to determine how endogenous APC association with MT ends affects plus-end dynamic instability and whether this requires its interaction with EB1. Because overexpression of MT binding proteins often promotes MT sta-

bilization in cells, and overexpression of APC can cause cell cycle arrest (Baeg *et al.*, 1995), apoptosis (Morin *et al.*, 1996), or disordered cell migration in tissue (Wong *et al.*, 1996), we developed a fluorophore-labeled anti-APC monoclonal antibody (mAb) as a nonperturbing tool to visualize the dynamics of endogenous APC in living cells. In conjunction with a spectrally distinct MT label, this enabled us to compare the dynamics of APC-decorated and undecorated MTs in the same cell. This analysis revealed novel behaviors of APC and also showed that MTs spent more time in the growth state while their plus ends were decorated with APC. Using an APC-deficient cell line and small inhibitory RNA (siRNA) inhibition of EB1 expression, we found that APC and EB1 could localize to MT ends independently of one another and that APC-decorated MT ends exhibited greater net growth than undecorated MTs, even in the absence of EB1.

MATERIALS AND METHODS

Antibodies and DNA

Anti-N-APC mAb (clone ALI12-28) was obtained from Cancer Research UK hybridoma bank/antibody services (London, United Kingdom). For immunolocalization of tubulin, two different mAbs, mouse monoclonal anti- α -tubulin (clone DM1 α ; Sigma-Aldrich, St. Louis, MO) or rat monoclonal anti-yeast tubulin (clone YL1/2; Serotec, Oxford, United Kingdom) were used. Anti-EB1 mAb was purchased from BD Transduction Laboratories (La Jolla, CA) (clone 5), and anti-EB1 rabbit polyclonal antibody was kindly provided by Dr. A. Barth (Stanford University, Palo Alto, CA). Human EB1/pEGFP-N1 (inserted into SacI and SmaI sites) was kindly provided by Dr. L. Cassimeris (Lehigh University, Bethlehem, PA). Human APC/pEGFP-C1 (inserted into BglIII and BamHI) was a kind gift from Drs. R. Rosin-Arbesfeld and M. Bienz (MRC Laboratory of Molecular Biology, Cambridge, United Kingdom).

Cell Culture

Madin-Darby canine kidney (MDCK) epithelial cells and mouse primary fibroblasts line 341 (wild type) and line 335 (APC deficient; carrying a mutation in exon 8 of APC gene that destabilizes APC mRNA (Kroboth, Newton, Kita, Li, Zumbunn, Waterman-Storer, and Nätke, unpublished data, origin; Dr. Robert Weinberg, Whitehead Institute, Cambridge, MA) were grown at 37°C and 5% CO₂ in high-glucose DMEM (Invitrogen, Carlsbad, CA) supplemented with 10% fetal bovine serum (Invitrogen for MDCK and Atlanta Biologicals [Norcross, GA] for mouse primary fibroblasts), 1/100 antibiotic/antimycotic (for MDCK), or 1/200 penicillin/streptomycin (for primary fibroblasts), 1 mM sodium pyruvate, 2 mM L-glutamine, minimal essential medium nonessential amino acids (all supplements were purchased from Invitrogen). MDCK cells were seeded onto collagen-coated coverslips and incubated for 2–4 h before experiments. For high-resolution live cell imaging, phenol red-free DMEM was used.

Preparation of Fluorescently Labeled Tubulin and mAb Probe

Both Alexa Fluor 488 and 568 carboxylic acid succinimidyl esters were purchased from Invitrogen. Alexa Fluor 488-tubulin was prepared according to Waterman-Storer (2002). To label the anti-N-APC mAb, the mAb was dialyzed into 20 mM HEPES buffer, pH 7.7, containing 150 mM NaCl at 4°C overnight, and concentrated to 1.0 mg/ml. Alexa Fluor 568 carboxylic acid succinimidyl ester was added at a molar ratio of 1:10 protein:dye to the sample solution with mixing. The coupling reaction was performed at room temperature for 1 h and terminated with 20 mM ethanolamine, pH 9.0. The labeled mAb was purified by gel filtration (GE Healthcare, Little Chalfont, Buckinghamshire, United Kingdom). Dye/protein ratio (=4.3) was calculated according to the manufacturer's protocol. The needle concentration of microinjected labeled mAb was ~100–140 μ g/ml.

Immunofluorescence Staining

For the localization of APC or EB1, culture media were removed, and cells were immediately fixed with -20°C methanol for 5 min. Cells were rehydrated in phosphate-buffered saline (PBS) for 5 min followed by blocking with 5% donkey serum in PHEM buffer (60 mM PIPES, 25 mM HEPES, 10 mM EGTA, and 4 mM MgSO₄, pH 7.2) to minimize nonspecific antibody absorption to the cells. The cells were incubated with the appropriate dilution of primary antibody in 5% donkey serum-PHEM buffer for 1 h (anti-tubulin mAbs, 1/500; anti-M-APC polyclonal, 1/1000; and Alexa Fluor 568-anti-N-APC and anti-EB1 mAb, 1/100), washed with PBS (5 min; 3 times). Labeling with a secondary antibody (Jackson ImmunoResearch Laboratories, West Grove, PA) followed in the same manner.

Coverslips were mounted on slides with 50% glycerol, 50% PBS containing *n*-propyl-gallate and sealed with nail polish.

Microscopy

Low-magnification phase-contrast movies were taken using an inverted microscope TE-200 (Nikon, Melville, NY) equipped with a 20 \times Plan Fluor phase lens (0.5 numerical aperture [NA]), a C4742-95 12G04 12-bit chilled charge-coupled device (CCD) camera (Hamamatsu Photonics, Hamamatsu, Japan), and a robotic MS-2000 XYZ microscope stage (Applied Scientific Instruments, Eugene, OR) equipped with linear positional feedback controllers (Haidenhain, Schaumburg, IL) on all three axes. Images were collected at 5-min intervals.

For spinning disk confocal imaging Alexa 568-labeled APC mAb and Alexa 488 tubulin in living cells, the sample was illuminated with either the 488 or 568 nm lines of a 2.5 W Kr/Ar laser, with the wavelength selected by a polychromatic acousto-optical modulator (Neos Technologies, Melbourne, FL). To avoid photobleaching, Oxyrase (Oxyrase, Mansfield, OH) was added to cell culture media at 30 μ l/ml. Digital images were acquired with a 14-bit C4742-48-24NR (OrcaII) CCD camera (Hamamatsu Photonics). Images were collected with a 100 \times 1.4 NA Plan Apo differential interference contrast (DIC) objective lens using an Ultraview spinning disk confocal scan-head (PerkinElmer Life and Analytical Sciences, Boston, MA) attached to a TE-300 inverted microscope (Nikon). Details of the microscope system are described in Adams *et al.* (2003). Pairs of spectrally distinct images were acquired at 5- to 6-s intervals. For total internal reflection fluorescence microscopy, 488- and 568-nm laser lines from a 50-mW Kr/Ar air-cooled ion laser (Melles Griot, Huntingdon, Cambridgeshire, United Kingdom) were introduced via a custom epi-illumination on a TE-2000 inverted microscope (Nikon) via an optical fiber. A 100 \times Plan Apo DIC (1.45 NA) objective lens (Nikon) was used to achieve to a critical angle of laser illumination at the coverslip/cell interface to generate an evanescent excitation field. Excitation wavelength was controlled with a polychromatic acousto-optical modulator (Neos). All other details are described in Adams *et al.* (2004). To acquire high-speed images, a 16-bit on-chip electron multiplier CCD camera, C9100-12 (Hamamatsu Photonics) was used. For all experiments, the stage temperature was controlled by an ASI 400 air stream incubator (Nevtek, Burnsville, VA).

Drug Perfusion during Live Cell Imaging

All perfusion equipment was purchased from Warner Instruments (Hamden, CT). Nocodazole-containing medium was perfused onto cells during high-resolution time-lapse imaging using an RC-30 chamber. Temperature was kept at 37°C by an SH-27B in-line solution heater and heater in the chamber, both were controlled by TC-344B dual-channel heater controller. Two minutes after taking a movie in nocodazole-free media, medium containing 100 nM nocodazole was perfused by electrically opening the valve with a VC-6 perfusion valve controller.

Analysis of MT Dynamics

The position of each MT end was tracked by hand using the "track points" function in MetaMorph software (Molecular Devices, Sunnyvale, CA), and data were transferred to Excel (Microsoft, Redmond, WA), followed by analyses with a custom-written macro (Wittmann *et al.*, 2003). Because the optical resolution limit is ~0.25 μ m, only length changes exceeding this threshold value were considered for MT dynamics analyses. Transition events from pause to shortening (or growth) were only classified as catastrophe (or rescue) if growth (or shortening) preceded the pause. The catastrophe (or rescue) frequency was defined as number of catastrophe (or rescue) events divided by the time the MT spent growing (or shortening) before the event.

Small Inhibitory RNA Interference

EB1-RNA interference (RNAi) experiments were conducted by expressing siRNA under the control of the polymerase-III H1-RNA gene promoter (Brummelkamp *et al.*, 2002). To allow location of RNAi-expressing cells by microscopy, we created the enhanced green fluorescent protein (EGFP)-RNAi vector. pEGFP-C3 (Clontech, Palo Alto, CA) was digested with SacI and SmaI to remove the multicloning site of the vector followed by religation. Then, the multicloning site-truncated vector was cut with DraIII. The pSUPER vector (Brummelkamp *et al.*, 2002) was digested with SacI and KpnI to obtain the H1-RNA promoter. The obtained 400-base pair fragment and the truncated pEGFP-C3 were filled in with Vent DNA polymerase (New England Biolabs, Beverly, MA) to create blunt ends. The truncated pEGFP-C3 was dephosphorylated, and the pSUPER-derived fragment was ligated into the vector. To specifically inhibit EB1 expression, the following sequence was inserted into the vector: 5'-GATCCCCGTGAATTCGAAGCTAAGCTTCAAGAGAGCTTAGCTTG-GAATTCACITTTTGGAAA-3'. Bold shows sense and underlined bold shows antisense sequence starting at 245 bp from the human EB1 initiation codon.

RESULTS

Alexa 568-labeled Anti-N-APC mAb as a Tool to Visualize Endogenous APC in Living Cells

Our first goal was to visualize APC in living cells in a nonperturbing way. Because even relatively low levels of exogenously expressed GFP-APC decorated many MTs and promoted MT bundling (Figure 1C and Movie 1), we were concerned that artifactual effects on MT dynamic instability might be induced by even mild protein expression. To alleviate this problem, we prepared a fluorescently labeled mAb against APC as a probe to follow endogenous APC in living cells, an approach that has been used successfully to monitor kinetochore dynamics (Maddox *et al.*, 2003). Because APC is a multifunctional protein with many binding sites for other proteins (Näthke, 2004), we chose an anti-APC mAb that recognizes an epitope in the N-terminal region of the protein that does not overlap with regions of the APC protein involved in Asef or KAP3 binding or the essential oligomerization domain (Figure 1A). The mAb was labeled with Alexa 568 dye and will be referred to as Ax568-N-APC. In fixed MDCK epithelial cells, immunostaining with Ax568-N-APC showed a localization pattern that was indistinguishable from that obtained with an anti-M-APC polyclonal antibody, with APC clusters at or near the ends of a small subset of MTs in cell extensions (Figure 1B) (Näthke *et al.*, 1996; Barth *et al.*, 2002). In addition, microinjected Ax568-N-APC followed by immunostaining showed that the injected mAb colocalized with endogenous APC in similar clusters (Figure 1, D–F).

APC has been proposed to play a role in epithelial cell migration and cell division (Wong *et al.*, 1996; Kaplan *et al.*, 2001; Jimbo *et al.*, 2002; Green and Kaplan, 2003). To verify that Ax568-N-APC antibodies did not affect these possible APC-mediated cell functions, we microinjected it into MDCK cells and monitored cell division and cell migration by time-lapse phase-contrast microscopy. To enrich for mitotic cells, the cell cycle was synchronized at G₂/M with 1 μ M nocodazole treatment, and Ax568-N-APC was microinjected soon after release from the nocodazole block. Because APC depletion or the expression of C-terminal truncated APC have been shown to have effects on kinetochore–MT plus-end attachment and chromosome alignment during prometaphase (Green and Kaplan, 2003; Green *et al.*, 2005), we specifically assayed the effects of Ax568-N-APC antibody on the time required for cells to transit from nuclear envelope breakdown to full alignment of all chromosomes at the mitotic metaphase plate. This analysis showed that in the next cell cycle after release from the block, antibody-injected cells and uninjected controls achieved metaphase chromosome alignment at the same rate (Movie 2 and Supplemental Table 1), and we found no obvious effects on production of lagging chromosomes. In contrast, mutations in or acute loss of APC in mice causes impaired enterocyte migration in intestinal tissue *in situ* (Mahmoud *et al.*, 1997; Sansom *et al.*, 2004), whereas depletion of APC protein in colorectal tumor cells in culture inhibits their migration *in vitro* in transwell assays (Kawasaki *et al.*, 2003). Therefore, we determined whether cell migration was altered in Ax568-N-APC-injected cells. Tracking the position of injected and control cells in 6-h time-lapse phase contrast movies showed that neither total distance of cell movement nor instantaneous cell velocity was different (Supplemental Table 2). Examination of these movies revealed no obvious differences in cell–cell adhesion or overall morphology in Ax568-N-APC-injected cells compared with controls. Thus, we conclude that Ax568-N-APC can be microinjected into cells without perturbing these putative APC-mediated cell functions.

Dynamics of Endogenous APC and MTs in Living Cells

The dynamic relationship between APC and MTs has been only inferred by imaging GFP-APC in living cells. To directly examine the dynamic behavior of endogenous APC relative to MTs in living cells, we comicroinjected Ax568-N-APC and Alexa 488-labeled tubulin into MDCK epithelial cells and captured pairs of images of the spectrally distinct probes at 5- to 6-s intervals over time on a multispectral spinning disk confocal digital microscope system (Adams *et al.*, 2003; Figure 2A and Movie 3). As previously shown by immunostaining (Näthke *et al.*, 1996), only a few (~4–15) of the MTs in the cell, all of which resided in protrusions, were decorated at their plus ends with small, nearly round clusters of Ax568-N-APC that were at or slightly above the ~270-nm resolution limit of the microscope (Figure 2A and Movie 3). This is in contrast to expressed GFP-APC, which forms larger peripheral clusters and often labels the lattices of MTs (Figure 1C). As previously suggested from GFP-APC imaging (Mimori-Kiyosue *et al.*, 2000a), the fluorescent clusters primarily associated with growing MT plus ends and often dissociated from MT ends when the MTs underwent a catastrophe, switching from growth to shortening (Figure 2B, arrowheads, and Movie 4). Very infrequently, we also observed a very dim resolution-limited APC signal moving toward the plus ends of peripheral MTs (our unpublished data), as reported previously for GFP-APC (Mimori-Kiyosue *et al.*, 2000a). In addition, there was a second small population (2–5) of Ax568-N-APC-labeled globular clustered structures that remained stationary near the edge of cellular protrusions without colocalization with MTs (Figure 2B, small arrows), and which seemed to dissolve over a few minutes time. These may represent the APC clusters that are thought to interact with the plasma membrane in an actin-dependent manner (Rosin-Arbesfeld *et al.*, 2001). In many cases, we could also observe that Ax568-N-APC formed small clusters on MT ends that were transferred and deposited to preexisting stationary Ax568-N-APC clusters near the cell edge (Figure 2B and Movie 4). In a few cells, there were also larger (3- to 5- μ m) vesicles of APC that moved rapidly along MTs in the central cytoplasm and likely represent accumulated antibody undergoing degradation in lysosomes that are moved on MTs via motor proteins.

To examine the specificity of Ax568-N-APC, we comicroinjected the antibody and Alexa 488 tubulin into APC-deficient mouse fibroblasts and their littermate wild-type fibroblasts (see *Materials and Methods*). Although the wild-type fibroblasts express less APC than MDCK cells (our unpublished data), we were able to visualize similar dynamics of the Ax568-N-APC in clusters on the smaller subset (2–6) of MT plus ends in cell protrusions, although the non-MT-associated stationary APC clusters were much less prominent than in MDCK cells (Figure 3A and Movie 5). In marked contrast to wild-type fibroblasts, in APC-deficient fibroblasts, we could not detect Ax568-N-APC clusters on distal ends of MTs or stationary clusters at the cell periphery (Figure 3B and Movie 6). However, we frequently observed the larger round fluorescent “lysosomal” structures moving along MTs in the cell center that were present in wild-type fibroblasts and MDCK cells. Together, these results confirm that the dynamic behavior of Ax568-N-APC on MT ends and in clusters in cell protrusions is similar to that observed for GFP-APC (Mimori-Kiyosue *et al.*, 2000a) and is not due to a nonspecific binding of the labeled mAb.

APC Clusters Associate with MT Plus Ends during Shortening

In addition to the previously reported behavior of APC described above, our analysis of endogenous APC labeled

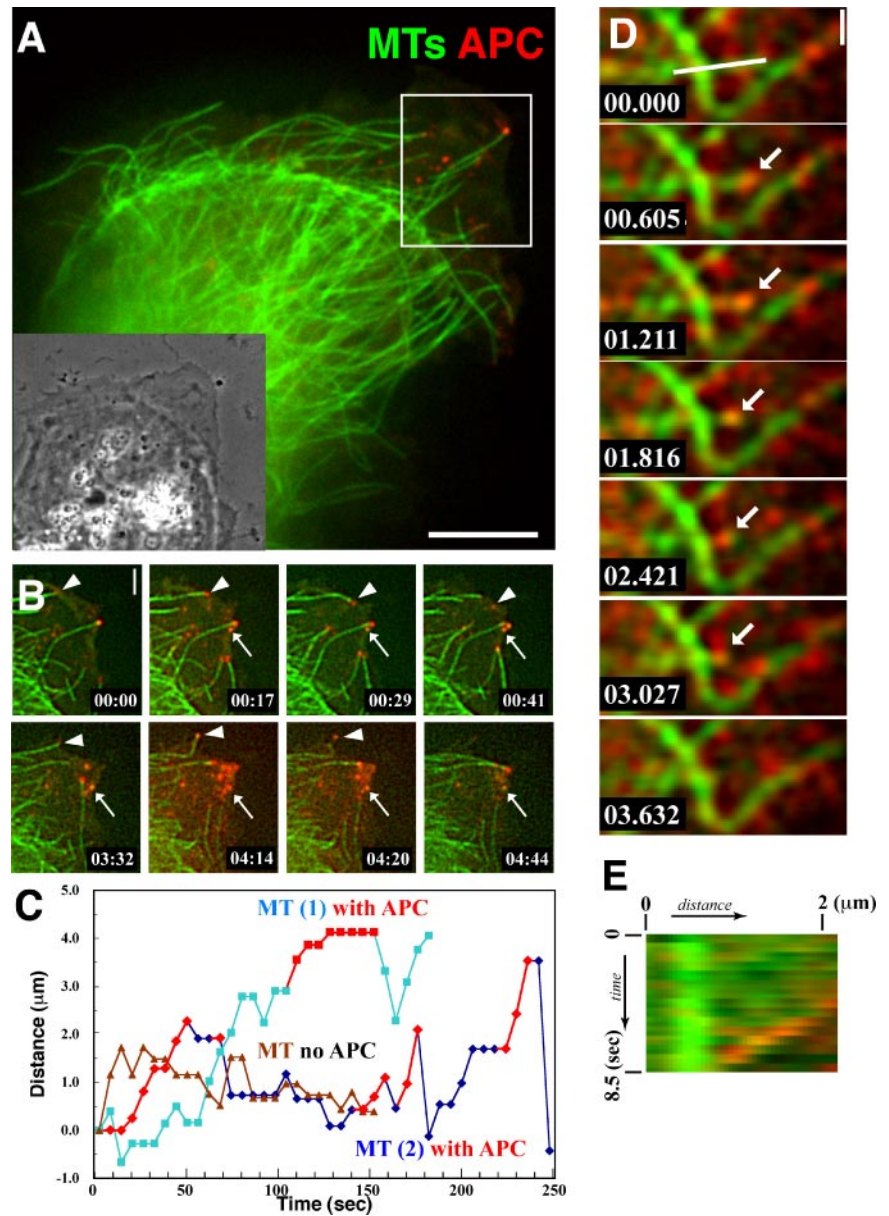


Figure 2. APC associates transiently with MT ends during all phases of dynamic instability. MTs (green) and endogenous APC (red) were visualized by microinjecting Alexa Fluor 488-tubulin and Alexa Fluor 568-anti-N-APC mAb together into MDCK cells, pairs of images of the two probes were captured over time, and the image pairs were color encoded and overlaid. (A) Spinning disk confocal image from the first frame of Movie 3; the inset shows the phase contrast picture of the same cell. Note that only a small subset of MTs concentrated near the leading edge have an APC cluster at their plus end. Bar, $8\ \mu\text{m}$. (B) Image series from the region delineated by the white box in A (Movie 4). APC clusters remain associated with growing MT plus ends, and the APC dissociates when the MT switches to shortening (arrowheads). APC clusters also remain stable in the cell protrusion in the absence of association with MT plus ends (small arrows). Bar, $2\ \mu\text{m}$. (C) Typical MT “life history plots” of the position of different MT plus ends in the same cell over time with and without bound APC. Time during APC-MT association is indicated by red symbols. (D) Total internal reflection fluorescence microscopy image series taken with a high-speed intensified CCD camera reveal the association of an APC cluster that remains associated with a shortening MT plus end (arrow). Also see Movie 5. Bar, $1\ \mu\text{m}$. (E) Dual-color kymograph of the region highlighted by a white line in D, showing the association of APC with a shortening MT over time.

with Ax568-N-APC and fluorescent MTs also revealed novel APC behaviors. Surprisingly, our dual-color movies revealed that Ax568-N-APC-labeled clusters seemed to remain associated with MT ends as the MT underwent shortening for up to 10–15 s (Movie 4). Because of limits in the illumination intensity and camera speed on our dual-wavelength spinning disk confocal system, the minimal time between Ax568-N-APC and Alexa 488 tubulin images was ~ 2.5 s. To confirm that the apparent association of APC with shortening MT ends was not due to a time resolution artifact, we used a combination of total internal reflection fluorescent microscopy to reduce fluorescence background and a high-speed intensified cooled CCD camera (see *Materials and Methods*). This allowed us to acquire pairs of spectrally distinct images at 600-ms intervals. This analysis confirmed the association of Ax568-N-APC clusters with shortening MT ends over several seconds and several microns of MT shortening (Figure 2, D and E, and Movie 7).

APC Stabilizes MTs by Promoting Growth, Slowing Shortening, and Decreasing Catastrophe and Rescue Frequencies

To determine how APC affects MT plus-end assembly/disassembly dynamics specifically during the time it is associated with MT ends, we compared the dynamics of APC-decorated and nondecorated MT plus ends in similar peripheral protrusions of the same cells. This was achieved by tracking MT plus-end position over time in dual-color movies, so that we could determine which MT ends were decorated with APC clusters and precisely the period of time of decoration. Figures 2C and 3C show typical life history plots of the position of MT plus ends over time for APC-decorated and nondecorated MT ends in MDCK and wild-type mouse primary fibroblasts, respectively, with the time of APC-MT end decoration highlighted in red. From measurements such as these, we calculated parameters of dynamic instability (see *Materials and Methods*) for non-

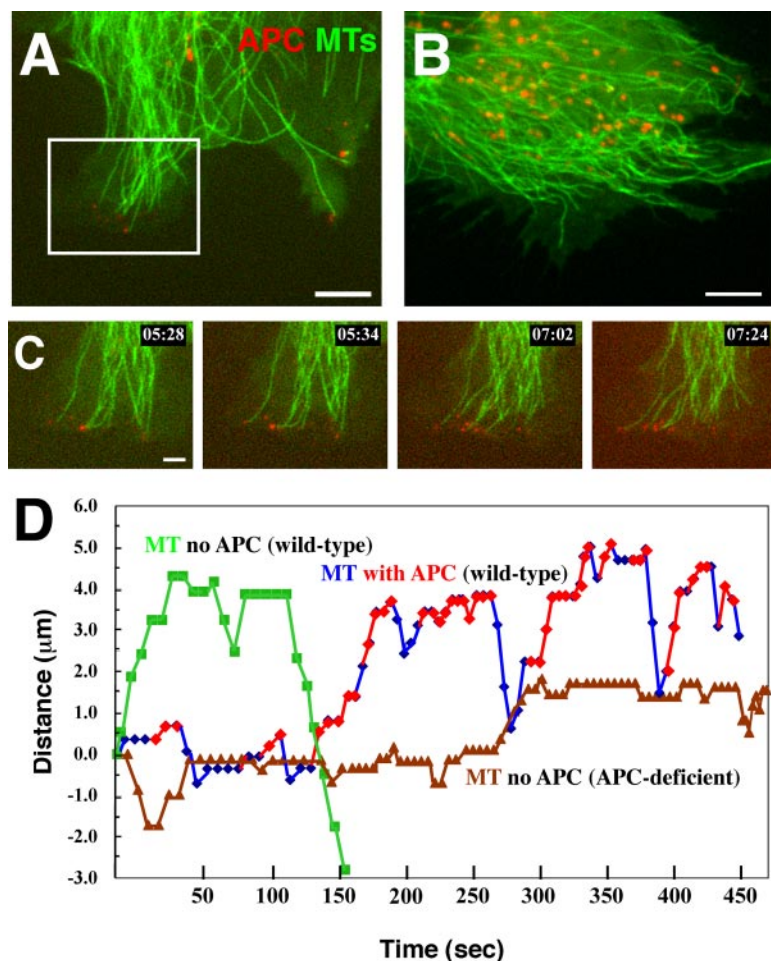


Figure 3. MTs (green) and Ax568-N-APC (red) in 341 (wild type; A) and 335 (APC deficient; B) mouse primary fibroblasts (Movies 6 and 7, respectively). Note that APC signal is neither detected at MT ends nor in peripheral clusters in the APC deficient cells in B. Red granule-like puncta in the cell center are likely nonspecific accumulation of the labeled mAb in lysosomes and can sometimes also be seen in MDCK cells in Figure 2A. Bars in A and B, 5 μm . (C) Magnified image sequence from the region delineated by the white box in A showing the association of APC on dynamic MT ends. Bar, 2 μm . (D) Typical life history plot of APC-decorated MTs (blue) versus non-APC-decorated MTs in wild-type (green) and APC-deficient (brown) cells. Time during APC-MT association marked by red symbols.

APC-decorated MTs in cellular extensions and for the portion of time when the MT end was decorated with APC. In MDCK cells, this analysis showed first of all that APC could decorate MT plus ends during all phases of dynamic instability including growth, shortening, and transitions between these states (catastrophe and rescue). Second, it revealed that during their time of APC decoration, MT ends had different parameters of dynamic instability than nondecorated MT ends in similar cell regions. Specifically, compared with nondecorated MT ends, MTs with APC on their ends spent more time in the growth phase, less time in the shortening phase, shortened slightly more slowly, and both their catastrophe and rescue frequencies were decreased (Table 1). The decreased shortening rate of APC-decorated MTs resulted in very short shrinking excursions compared with non-APC-decorated MTs (Table 2).

Because we found that APC associates with MTs in all phases of dynamic instability, we wanted to determine the phase when APC clusters dissociate from MT ends. By analyzing dual-color movies, we found that half of the APC-MT end dissociation events occurred during catastrophe. Interestingly, we also observed APC clusters dissociating from MT ends during growing, shortening or pausing (Table 3). No example of APC-MT dissociation during MT rescue was observed.

To confirm that APC stabilization of MT plus-end growth occurred in other cell types, we performed the same analysis using wild-type mouse primary fibroblasts (Movie 5). Because the amount of endogenous APC protein in these fibroblasts is less than in MDCK epithelial cells and the APC-

decorated MT ends tend to accumulate together at extensions of cell edges, it was difficult to analyze a large sample of APC-decorated MTs. In spite of this, we observed the same tendency as in MDCK cells, with APC-decorated MT ends spending more time in growth and less time in shortening than non-APC-decorated MT ends and shortening more slowly (Table 1), again resulting in limited shortening excursion lengths (Table 2). In addition, in fibroblasts, both the catastrophe and rescue frequencies of APC-decorated MTs were half that of the undecorated MTs, a more substantial difference than in MDCK cells (Table 1). Together, these results show that during the time that APC associates with MT plus ends, the ends undergo net growth by increasing the time spent growing, decreasing the time and speed of shortening and decreasing the frequency of switching between growth and shortening states.

To determine whether APC has effects on MT dynamics distinct from its association with MT ends, we compared the dynamics of non-APC-decorated MTs in wild-type mouse primary fibroblasts to MTs specifically in peripheral extensions of APC deficient fibroblasts in cells coinjected with Ax568-N-APC and Alexa 488 tubulin. Examination of time-lapse image series and quantitation of dynamic instability parameters revealed no substantial differences between these MT populations (Table 1). This indicates that the effects of APC on MT dynamic instability is specifically due to its association with the MT plus end and not due to an APC-dependent indirect regulatory mechanism.

Table 1. Parameters of MT dynamic instability for APC-decorated and non-APC MTs in MDCK, wild-type, and APC-deficient mouse primary fibroblasts

	MDCK		341 (wild-type)		335 (APC-null)
	APC-decorated MTs	Non-APC MTs	APC-decorated MTs	Non-APC MTs	Non-APC MTs
Growth rate ^a					
Mean ($\mu\text{m}/\text{min}$)	4.34 \pm 1.91 (164)	3.88 \pm 1.66 (552)	5.75 \pm 4.73 (44)	5.35 \pm 3.12 (400)	6.08 \pm 5.62 (338)
Median ($\mu\text{m}/\text{min}$)	3.83	3.36	3.83	4.21	4.89
Shortening rate ^a					
Mean ($\mu\text{m}/\text{min}$)	-4.05 \pm 2.07 (43)	-6.03 \pm 4.58 (415)	-3.73 \pm 0.70 (6)	-9.27 \pm 7.86 (198)	-7.45 \pm 5.62 (222)
Median ($\mu\text{m}/\text{min}$)	-3.06	-4.25	-3.89	-6.25	-5.47
Total events of catastrophe	32	251	14	134	124
Total events of rescue	30	244	11	121	116
Catastrophe frequency (s^{-1})	0.0105	0.0140	0.0092	0.0212	0.0182
Rescue frequency (s^{-1})	0.0098	0.0136	0.0092	0.0191	0.0170
Time spent for					
Growing (%)	31.4	18.1	48.0	38.2	30.5
Shortening (%)	8.3	13.8	6.5	19.9	20.5
Pausing (%)	60.3	68.1	45.5	41.9	50.6
Total time observed (min)	51.0	298.7	17.2	105.3	113.6
No. of cells, microtubules	10, 36	13, 77	6, 11	7, 29	6, 33

^a Number of events is given in parentheses.

APC-EB1 Colocalization Is Spatiotemporally Restricted

APC (Su *et al.*, 1995) and other +TIP proteins (Askham *et al.*, 2002; Ligon *et al.*, 2003; Mimori-Kiyosue *et al.*, 2005) can biochemically interact with EB1, a well characterized +TIP that may promote MT dynamic instability (Rogers *et al.*, 2002; Tirnauer *et al.*, 2002). Thus, we sought to determine whether the effects of APC we observed on MTs were related to its colocalization with EB1. To characterize the relationship between EB1 and APC, we first conducted immunostaining to determine the degree of colocalization of the two proteins. Because the anti-EB1 mAb we obtained stained MDCK cells poorly in our hands, we evaluated wild-type mouse primary fibroblasts (Figure 4, A–D). Triple immunofluorescence localization of EB1, MTs, and APC showed that the two proteins had distinct distributions, with EB1 forming comet-shaped structures at the ends of many MTs throughout the cell that colocalized with only a very minute number of (1–4) spherical APC clusters at MT ends in cell protrusions as shown previously in MDCK cells (Barth *et al.*,

2002). This shows that the colocalization of APC and EB1 is very spatially restricted and suggests it may be a transient event.

To confirm this, we simultaneously imaged the dynamics of APC and EB1 in living cells. Here, our Ax568-N-APC mAb allowed us to conduct dual-color imaging of endogenous APC in a MDCK cell line stably expressing EB1-GFP, that does not perturb MT plus-end growth dynamics in cells when overexpressed at low levels (Piehl and Cassimeris, 2003). Because ectopically expressed EB1 can promote MT bundling and recruit APC (Mimori-Kiyosue *et al.*, 2000b), we compared the expression level of EB1-GFP with endogenous EB1 (Supplemental Figure 1A, EB1-GFP = 200% of endogenous EB1) and also confirmed the normal distribution of endogenous APC and MTs in these cells by immunostaining (our unpublished data). Live cell imaging of EB1-GFP and endogenous APC using Ax568-N-APC showed that many EB1 comets moved throughout the cell, and only a very small number of the comets transiently colocalized with APC clusters. EB1 comets could generally be seen moving from central cell regions toward the periphery, and only when the comet continued to move within ~5–7 microns from the edge of cell protrusions did the comet acquire an additional APC cluster at its tip (highlighted comet in Figure 5). When a peripheral EB1 comet disappeared (suggesting that the growing MT switched to shortening), the APC cluster often was left behind at the site of EB1 disappearance (Figure 5 and Movie 8). In addition, once EB1 comets neared the cell periphery, they often contacted preexisting MT-independent cortical APC clusters. Although the majority of EB1 comets in the cell were not colocalized with APC clusters, nearly all APC clusters were at some point in their lifetime contacted at least transiently with EB1 comets. These results show that the colocalization of EB1 and APC is a very spatiotemporally restricted event that occurs only for a very brief time in peripheral cell extensions.

EB1 and APC Localization to MT Ends in Cell Protrusions Are Independent






Because both EB1 (Su *et al.*, 1995) and APC (Smith *et al.*, 1994) not only bind directly to MTs but also indirectly associate

Table 2. Effect of APC-MT interaction on excursion length of MTs in MDCK and mouse primary fibroblasts

	APC decorated		Non-APC MTs	
	Growth	Shortening	Growth	Shortening
MDCK				
μm	0.812	-0.440	0.758	-0.878
Increase or decrease (%)	107.1	50.1	100	100
Wild-type mouse primary fibroblast				
μm	1.763	-0.790	1.530	-1.414
Increase or decrease (%)	115.2	55.9	100	100

Each value shows the average. Percentage of increase or decrease shows the change against the same category of non-APC MTs.

Table 3. APC dissociation from MT ends during different phases of dynamic instability

					
	Catastrophe	Rescue	Growing	Shrinking	Pausing
MDCK (n, %)	50, 49.5	0, 0	15, 14.9	14, 13.9	22, 21.8
Wild-type fibroblast (n, %)	9, 52.9	0, 0	6, 17.6	6, 17.6	5, 14.7

with MTs by binding to one another, we sought to determine whether their associations with MT ends in peripheral cell protrusions were interdependent. To determine whether APC localization to MT ends was dependent on EB1, we inhibited EB1 expression by RNAi in mouse primary fibroblasts and determined the localization of APC in fixed cells. Including a GFP expression cassette in the RNAi vector (see *Materials and Methods*) allowed us to determine the efficiency of transfection, which was 50–70%. Immunoblot analysis of transfected cells revealed a 75% reduction of EB1 protein, which bottomed out at 2 d after transfection (Supplemental Figure 1, B and C). Immunostaining with anti-EB1 antibody

revealed that transfected cells had significantly reduced EB1 protein levels, with no comet structures at MT ends and only background punctate staining (Figure 4). We found no difference in the localization of APC to clusters near MT ends in peripheral cell protrusions in EB1-depleted cells compared with wild-type fibroblasts not subjected to EB1 RNAi (Figure 4, I–L), indicating APC does not require EB1 for its normal localization.

To determine whether EB1 can localize to MT plus ends in cell protrusions independent of its association with APC, we compared immunostaining in wild-type and APC-deficient mouse primary fibroblasts. As shown in Figure 4, E–H, this

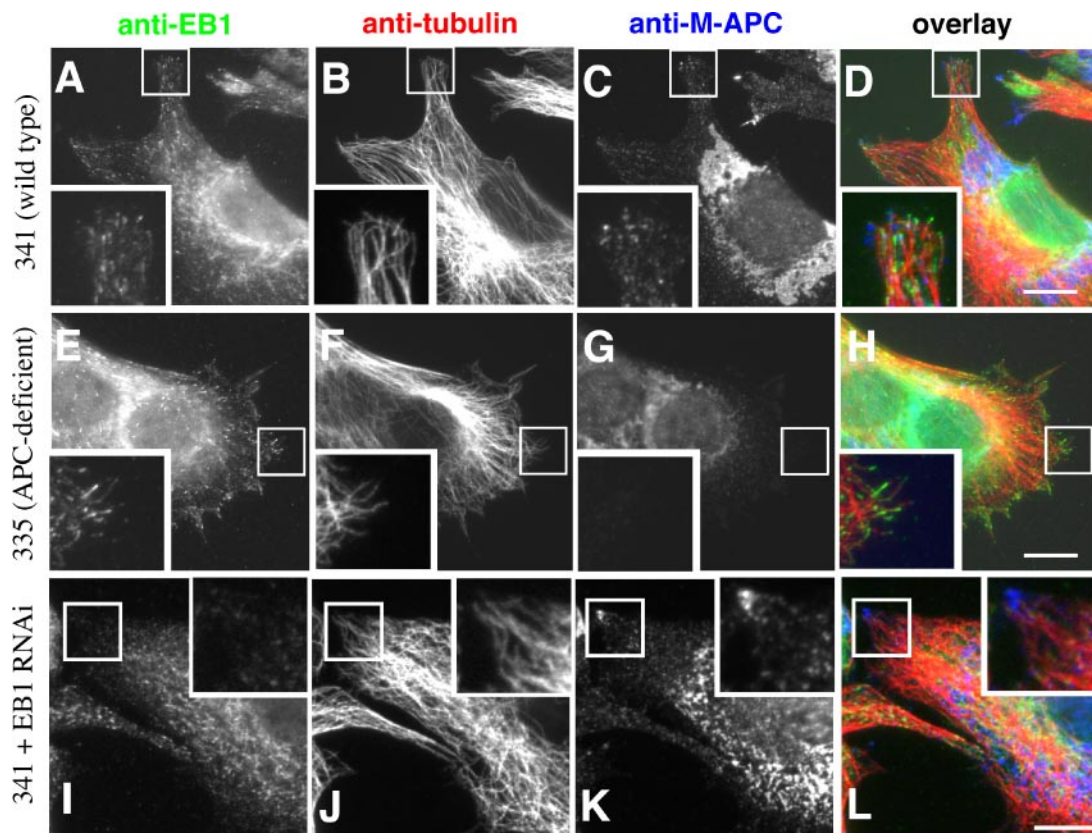


Figure 4. EB1 and APC subcellular localizations are independent. (A–D) 335 (APC-deficient) primary mouse fibroblast. (E–H) 341 (wild-type) primary mouse fibroblast. (I–L) 341 fibroblasts expressing double-stranded RNA to inhibit translation of EB1. (A, E, and I) Anti-EB1 immunofluorescence. (B, F, and J) Anti-tubulin immunofluorescence. (C, G, and K) Anti-M-APC immunofluorescence. (D, H, and L) Color overlay with EB1 in green, MTs in red, and APC in blue. Insets in all images show the magnified region indicated by the boxed area in the same panel. APC deficiency does not affect the MT plus end localization of EB1 (compare A–D to E–H). RNAi inhibition of EB1 protein expression level does not change APC localization to clusters in cell protrusions (E–H and I–L). Note that the anti-M-APC antibody produces a nonspecific perinuclear staining that is present in wild-type, APC-deficient, and EB1-deficient fibroblasts. Bars in D, H, and L, 10 μ m.

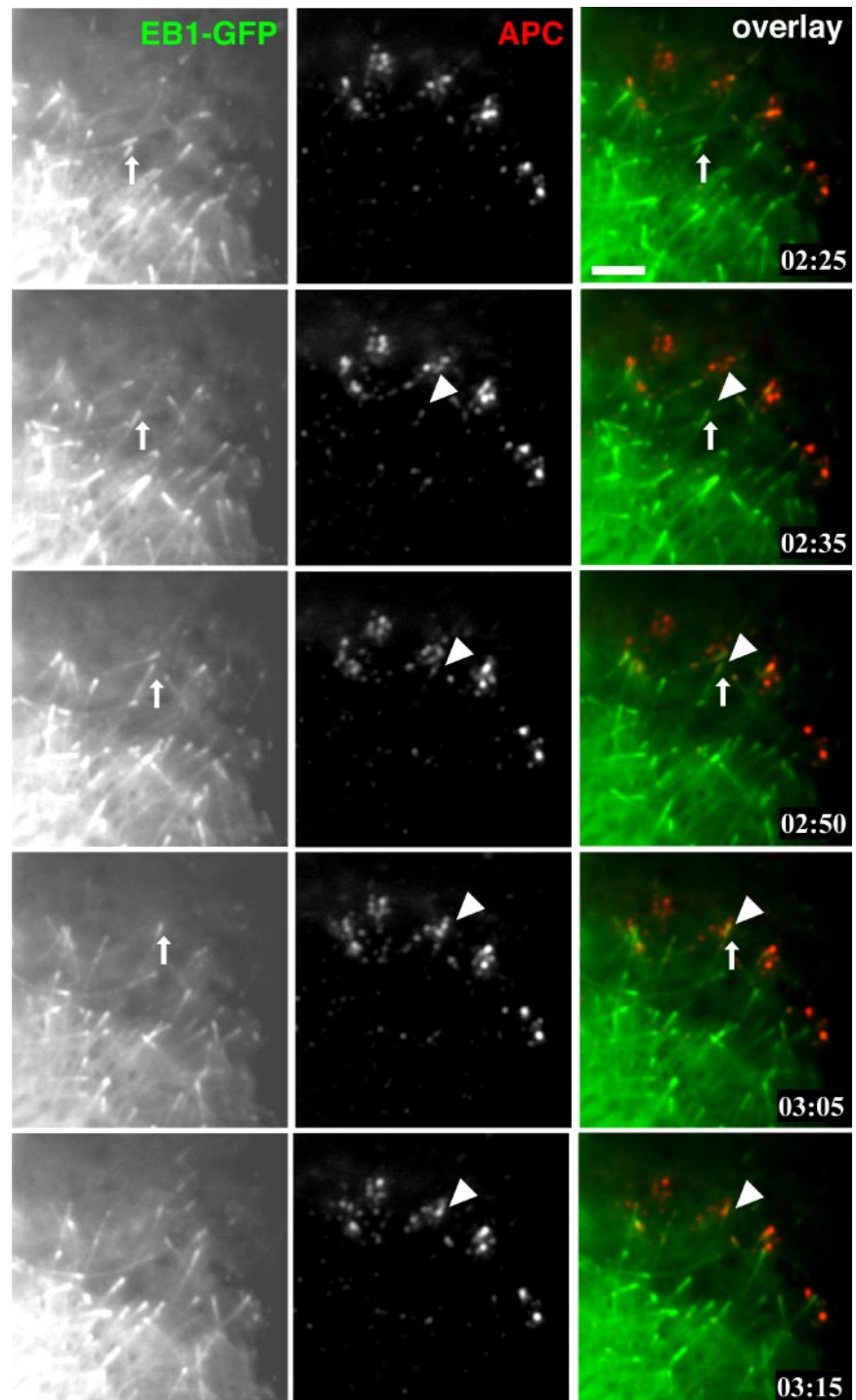


Figure 5. APC and EB1 colocalization is a spatiotemporally restricted event. Ax568-N-APC mAb was microinjected into MDCK cells stably expressing EB1-GFP, and total internal reflection fluorescent images were collected 3 h after microinjection (Movie 8). Many EB1 comets lack associated APC, and many APC clusters lack associated EB1; however, a small population of the two structures colocalize (arrow for EB1 and arrowhead for APC) for a short time during the later phases of a MT growth excursion. Bar, 3 μ m.

showed that in the absence of APC, EB1 still localized to comet structures on MT plus ends in peripheral cell extensions. Together, these results confirm that EB1 and APC can independently localize to MT plus ends.

APC on Microtubule Plus Ends Promotes Their Net Growth without EB1

To approach the question of whether the effects of APC association with MT plus ends on MT dynamic instability that we observed (Table 1) required EB1, we performed live

imaging of endogenous APC and MTs in mouse fibroblasts where EB1 was depleted by RNAi. Two days after transfection of the EB1-RNAi expression vector, Alexa 488-tubulin and Ax568-N-APC mAb were comicroinjected into cells followed by live imaging with dual-wavelength spinning disk confocal microscopy. Although the RNAi vector drove the expression of GFP to allow identification of transfected cells, the Alexa 488-tubulin signal was much stronger than the soluble GFP, making it still possible to measure MT dynamics. After live imaging, the cells were immediately fixed, and

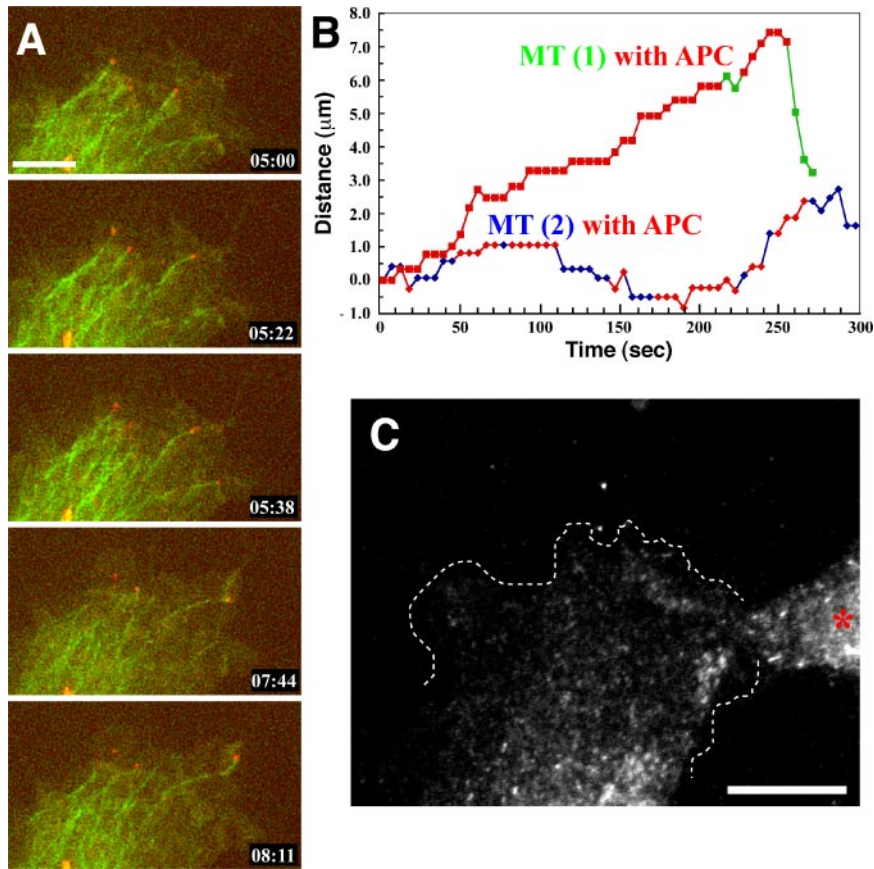


Figure 6. APC dynamic behavior is independent of EB1. (A) Time-lapse spinning disk confocal image series of Ax568-N-APC (red) and Ax 488 MTs (green) in an EB1-RNAi-expressing wild-type mouse primary fibroblast (Movie 9). Endogenous APC exhibits dynamic interactions with MT plus ends in the absence of EB1. Bar, 5 μm . (B) Examples of MT life history plots for APC-decorated MTs in cells expressing EB1-RNAi. Times of APC association are indicated by red symbols. (C) After time-lapse filming of the cell in A, the cell was fixed and EB1 was immunolocalized. The outline of the cell is shown with a dotted white line. This cell lacks EB1 comets, whereas the neighboring cell (asterisk) that was not expressing the EB1-siRNA construct clearly displays EB1 comets, indicating that the cell in A had reduced EB1 expression. Bar, 10 μm .

anti-EB1 immunostaining was performed to confirm the depletion of EB1 in the analyzed cell. Dual-color movies showed that in EB1-depleted cells, APC continued to decorate MT ends in living cells (Figure 6A and Movie 9), confirming the results in fixed cells (Figure 4, I–L). The plus ends of APC-decorated and nondecorated MTs in EB1-depleted cells were tracked

(Figure 6B), and dynamic instability parameters were calculated for periods during APC decoration and compared with APC-decorated and nondecorated MT ends in cells containing EB1 (Table 4). This analysis showed that both APC-decorated and non-APC-decorated MTs in EB1-depleted cells spent more time in pause and less time in growth compared with

Table 4. Parameters of dynamic instability for APC-decorated and non-APC MTs in EB1-depleted wild-type mouse primary fibroblasts

	EB1-RNAi		Control (from Table 1)	
	APC-decorated MTs	Non-APC MTs	APC-decorated MTs	Non-APC MTs
Growth rate				
Mean ($\mu\text{m}/\text{min}$) ^a	4.98 \pm 2.23 (66)	5.13 \pm 2.99 (193)	5.75 \pm 4.73 (44)	5.35 \pm 3.12 (400)
Median ($\mu\text{m}/\text{min}$)	4.43	4.42	3.83	4.21
Shortening rate				
Mean ($\mu\text{m}/\text{min}$) ^a	-4.80 \pm 3.16 (11)	-6.84 \pm 5.22 (123)	-3.73 \pm 0.70 (6)	-9.27 \pm 7.86 (198)
Median ($\mu\text{m}/\text{min}$)	-3.63	-4.93	-3.89	-6.25
Total events of catastrophe	9	63	14	134
Total events of rescue	10	64	11	121
Catastrophe frequency (s^{-1})	0.0094	0.0132	0.0092	0.0212
Rescue frequency (s^{-1})	0.0103	0.0134	0.0092	0.0191
Time spent for				
Growing (%)	37.5	23.6	48.0	38.2
Shortening (%)	6.2	15.0	6.5	19.9
Pausing (%)	56.3	61.4	45.5	41.9
Total time observed (min)	16.2	79.4	17.2	105.3
No. of cells, microtubules	6, 15	6, 22	6, 11	6, 27

^a Number of events is given in parentheses.

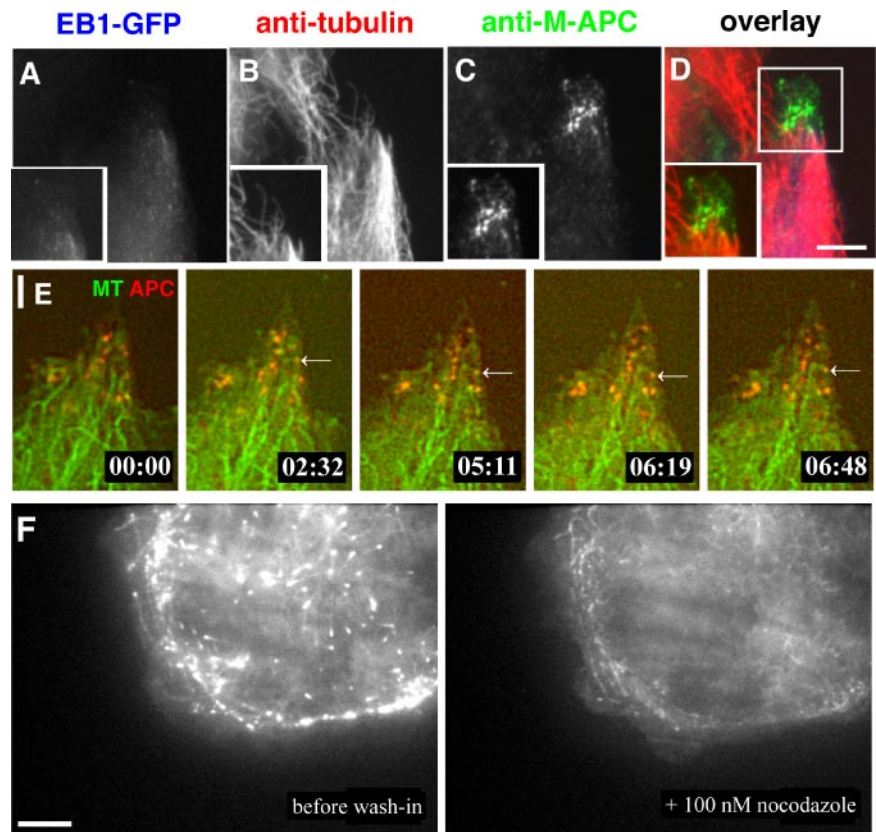


Figure 7. EB1 requires MT growth for plus-end localization, whereas APC does not. (A–D) MDCK cell stably expressing GFP-EB1 (A) were treated with 100 nM nocodazole for 15 min to inhibit MT plus-end assembly/disassembly dynamics, fixed, and MTs (B) and APC (C) were immunolocalized. The density of MTs is indistinguishable from untreated cells (i.e., see Figure 4) and APC clusters still localize near the plus ends of MTs in cell protrusions; however, EB1 comets at MT plus ends are absent. Bar, 3 μm . (E) Spinning disk confocal image series of Ax568-N-APC (red) and Ax488 tubulin (green) in an MDCK cell treated with 100 nM nocodazole. MT plus ends neither grow nor shorten, yet APC clusters remain in tight association with plus ends (arrow) (Movie 10). Bar, 2 μm . (F) Total internal reflection fluorescence images of a GFP-EB1 expressing MDCK cell before (left) and after (right) perfusion of 100 nM nocodazole. EB1 comets quickly disappear after wash-in of nocodazole (Movie 11). Bar, 5 μm .

APC-decorated and non-APC-decorated MTs in control cells. This is in agreement with previous studies of EB1 depletion in *Drosophila* S2 cells (Rogers *et al.*, 2002) and supports the notion that EB1 promotes MT assembly/disassembly dynamics in an APC-independent manner. However, in both EB1 depleted and control cells, APC-decorated MTs spent more time in the growth phase than non-APC-decorated MTs. EB1 depletion had no effect on the frequencies of MT plus end catastrophe and rescue for APC-decorated MTs (Table 4). However, EB1 depletion reduced the plus-end catastrophe and rescue frequencies of non-APC-decorated MTs compared with controls, although not to the same extent as the reduced transition frequencies observed for APC-decorated MTs compared with non-APC-decorated MTs in cells containing EB1. Together, these results suggest that endogenous APC decoration of MT plus ends promotes MT net growth and stabilization and that this effect can to some extent override the transition-promoting activity of EB1.

APC and EB1 Associate with MT Plus Ends via Distinct Mechanisms

Because APC and EB1 can localize to MT ends in cell protrusions independently (Figures 4, A–H, and 5), we suspected that different mechanisms govern the interaction of APC and EB1 with MTs. To test this idea, we applied nocodazole at submicromolar concentrations to cells to inhibit dynamic instability of MTs (Liao *et al.*, 1995) and then examined the association of EB1 and APC with the resulting nondynamic MT ends. EB1-GFP-expressing MDCK cells that were fixed and immunostained with anti-tubulin and anti-M-APC antibodies after a 15-min treatment with 100 nM nocodazole did not exhibit obvious changes in the overall organization of MTs (Liao *et al.*, 1995). Surprisingly, APC

clusters were still prominent and colocalized with MT ends in the periphery of cell extensions in nocodazole-treated cells (Figure 7, C and D). In contrast, in EB1-GFP-expressing MDCK cells treated similarly with nocodazole, EB1-GFP was diffuse in the cytosol and no longer associated with MT ends (Figure 7, A and D).

When living MDCK cells microinjected with Ax568-N-APC and Alexa 488-tubulin were subjected to time-lapse imaging in the presence of 100 nM nocodazole, we found that plus-end MT growth and shortening dynamics were indeed inhibited (Liao *et al.*, 1995), as shown in the sequential images of Figure 7E and Movie 10. However, we still observed colocalization of APC clusters to MTs ends that were in a state of pause. These APC clusters must be maintained in a MT-dependent manner because peripheral APC clusters disappeared after MT depolymerization by a higher concentration (10 μM) of nocodazole (Supplemental Figure 2). In contrast, the plus-end accumulation of EB1-GFP quickly disappeared after perfusion of 100 nM nocodazole to inhibit dynamic instability of MTs (Figure 7A and Movie 11). However, this often induced a low level of labeling along the entire MT-lattice with EB1-GFP. Together, these results clearly indicate that EB1 and APC use different mechanisms for localizing to MT plus ends in mammalian cells.

DISCUSSION

A Novel Probe to Examine the Dynamics of Endogenous APC

In this study, we established a fluorescently labeled mAb to APC as a nonperturbing probe to visualize the dynamics of endogenous APC in living cells. A similar approach has been used to analyze dynamics of kinetochores (Maddox *et al.*, 2003). The significance of this method for APC is that it can eliminate

the possible artifactual alteration of MT dynamics induced by even slight overexpression of GFP-tagged APC protein constructs. In addition, the fluorophore used is extremely bright and photostable compared with GFP, allowing visualization of the low level of endogenous APC for many image exposures. When microinjected into cells together with a spectrally distinct fluorescent tubulin analog, this allowed for the first time a direct characterization of the dynamic relationship between APC and MTs. The antibody used in this study reacts with epitopes outside the known protein-protein interaction domains of APC as well as those important for cytoskeletal-MT interaction. This antibody recognizes APC in mouse, dog (this study) and human (our unpublished data), making it a useful reagent for cells from different species. In addition, when microinjected, the labeled mAb did not disrupt putative APC-mediated functions, including chromosome alignment during mitosis and cell migration. Although this suggests that the mAb is nonperturbing, we cannot exclude the possibility that other APC-mediated functions are affected, such as β -catenin regulation or its transport by kinesin motors. However, this is unlikely based on the location of the epitope, and the recent demonstration that this anti-N-APC mAb can immunoprecipitate with the KIF3 associated molecule KAP3 in an endogenous APC-KAP3 complex (Li and Näthke, 2005). Some concern may exist that microinjected Ax568-N-APC mAb may label aggregates as reported recently (Riess *et al.*, 2005); however, we observed peripheral APC clusters in all cells examined, whereas aggregates are only observed during recovery from nocodazole treatment (Riess *et al.*, 2005). Thus, we conclude that the labeled mAb is a useful tool to analyze the effects of endogenous APC on the dynamics of the small subset of MT plus ends in interphase cells it decorates. This may also be useful to study other aspects of APC dynamics such as in the mitotic spindle.

+TIPs Exhibit Heterogeneous Behaviors

Simultaneous imaging of MTs and endogenous APC revealed the surprising and novel finding that APC remained associated with MT plus ends during all phases of dynamic instability, including growth, shortening, and the transitions between these states, and that APC could dissociate from MT ends during all phases except rescue. Other +TIPs characterized so far in vertebrate cultured cells are thought to associate only with growing MT plus ends and disappear when MT ends switch to shortening (Akhmanova and Hoogenraad, 2005). +TIPs seem to “move” with growing plus ends, but in fact they bind with high-affinity very close to growing plus ends, remain stationary with respect to the MT lattice, and exhibit an exponential decay in MT association with increasing distance from the plus end, suggesting first order dissociation kinetics (Tirnauer *et al.*, 2002; Wittmann and Waterman-Storer, 2005). This gives rise to the typical “comet” appearance and the “treadmilling” behavior of +TIPs. It has been demonstrated that CLIP-170 achieves this by binding to tubulin dimers and copolymerizing with tubulin into MT ends (Diamantopoulos *et al.*, 1999; Folker *et al.*, 2005). We found here that APC remained associated with MT ends during inhibition of MT assembly/disassembly dynamics with low concentrations of nocodazole, suggesting that APC does not associate with MT ends by copolymerization with tubulin.

APC has previously been differentiated from other +TIPs by the fact that it forms a round cluster at MT ends as opposed to a comet; it moves along the MT lattice toward plus ends; and when it dissociates from plus ends, the clusters remain stable for some time (Mimori-Kiyosue *et al.*, 2000a). Here, we additionally found that APC can remain

associated with or dissociate from MTs during many phases of dynamic instability. Interestingly, Bik1, the CLIP-170 homologue in budding yeast, has also been reported to remain associated with shrinking and pausing MTs (Carvalho *et al.*, 2004) and EB1 can localize to the ends of detyrosinated MTs that could be nondynamic (Wen *et al.*, 2004). Thus, +TIPs are a complex class of proteins with heterogeneous behaviors with respect to MT end dynamics.

The APC-EB1 Colocalization Is Very Limited In Vivo

Studies over the past several years have shown that many +TIP proteins have the capability to interact with one another, implying the existence of a MT +TIP complex (Allan and Näthke, 2001; Mimori-Kiyosue and Tsukita, 2003; Akhmanova and Hoogenraad, 2005). This has suggested that the functions of +TIP proteins may be interdependent, and makes it difficult to interpret effects of perturbation of single +TIP proteins. Here, we showed using dual wavelength live-cell imaging that APC and its binding partner identified by yeast two-hybrid, EB1 (Su *et al.*, 1995), colocalize only at a very limited subset of MT ends, and there the colocalization is very transient, suggesting that their interaction is extremely restricted. Using deficient cell lines and RNAi-mediated expression inhibition, we found that these two proteins localize to MT plus ends independently in tissue cells. Indeed, evidence from previous studies corroborates our findings that the APC-EB1 colocalization may be limited and not necessary for the localization of APC in mammalian cells. EB1 and APC localization were shown to be only partially coincident (Barth *et al.*, 2002), and EB1 distribution was not altered in a colon cancer cell line that expresses a truncated form of APC (Morrison *et al.*, 1998). In addition, it was recently found that APC can localize to the centrosome in an EB1-independent manner (Louie *et al.*, 2004). Furthermore, APC homologues of *Drosophila*, D-APC and E-APC, both lack an EB1 binding domain (Yu *et al.*, 1999), so at least *Drosophila* does not require a direct interaction between APC and EB1 for APC function. However, it has been reported that EB1 and APC work together to regulate spindle positioning and chromosome alignment during mitosis in tissue cells (Green *et al.*, 2005) and to presumably “cap” (Infante *et al.*, 2000) nocodazole-resistant MTs in interphase cells in response to lysophosphatidic acid stimulation (Wen *et al.*, 2004). Together, these studies suggest that the EB1-APC interaction may be important for a limited subset of APC functions.

APC Promotes Net MT Growth into Cell Extensions

Based on APC's decoration of a subset of MT ends in cell protrusions (Näthke *et al.*, 1996) and its promotion of MT stabilization when overexpressed in cells (Zumbrunn *et al.*, 2001), it has been hypothesized that APC may promote the local stabilization of MTs in the protrusions of cells. Here, we provide evidence for the effects of APC on MT assembly/disassembly dynamics in vivo by a direct comparison between the dynamics of the small subset of MTs with APC on their plus ends to neighboring MTs in the same cell that lack associated APC. As summarized in Table 1, we found in fibroblasts and epithelial cells that during the time that APC associates with MT plus ends, these ends are biased toward growth by increasing the time spent growing, decreasing the time and speed of shortening and decreasing the frequency of switching between growth and shortening states. Thus, APC association with MTs in cell protrusions promotes their net growth.

Our demonstration that endogenous APC can promote net MT growth into cell extensions, together with the hy-

pothesized role of APC in intestinal epithelial cell migration (Näthke, 2004) suggests that APC may contribute to the stabilization of MTs toward the protruding leading edge of migrating cells. Indeed, APC has been implicated in the formation of nocodazole-resistant MTs (Wen *et al.*, 2004), recognized by their posttranslational detirosination, that emanate toward the leading edge in migrating fibroblasts, whereas APC inhibition reduces MT length in semi-intact MDCK cells (Reilein and Nelson, 2005). Previous articles indicated that APC stabilizes and promotes the growth of MTs in vitro (Munemitsu *et al.*, 1994; Zumbunn *et al.*, 2001). APC is thus a good candidate for mediating the net growth of "pioneer" MTs in the lamella of migrating epithelial cells (Waterman-Storer and Salmon, 1997; Wadsworth, 1999). In addition to APC, MTs in cell protrusions may be stabilized by other factors, because we often observed that MTs could have prolonged growth excursions before their association with APC. Thus, leading edge MT stabilization may be the product of local regulation of several protein activities, including APC, Op18/stathmin, and CLASPs (Wittmann *et al.*, 2003, 2004; Wittmann and Waterman-Storer, 2005). Whether the stabilization of leading edge MTs by APC is required for directed cell migration remains to be determined.

The Role of EB1 in APC Regulation of MT Assembly/Disassembly Dynamics

By comparing the dynamics of APC-decorated and non-APC-decorated MTs in control and EB1-depleted cells, we found that APC could stabilize the growth of a subset of MTs independent of EB1. In both budding yeast (Tirnauer *et al.*, 1999) and *Drosophila* S2 cells (Rogers *et al.*, 2002), EB1 depletion increases paused MTs in interphase; therefore, EB1 is thought to promote MT assembly/disassembly dynamics in these cells. Similarly, we found for both APC-decorated and nondecorated MTs a trend toward increases in pause time when EB1 was depleted. However, APC-decorated MTs in both EB1-depleted and control cells spent more time in growth compared with non-APC-decorated MTs, indicating that APC can stabilize the growth state irrespective of its association with EB1. This agrees with previous studies in vitro that showed the ability of purified APC to promote the bundling and stability of MTs in vitro (Munemitsu *et al.*, 1994; Zumbunn *et al.*, 2001). Although Nakamura *et al.* (2001) reported that the APC-EB1 interaction is necessary to promote MT polymerization, they used only the C terminus of APC (a.a. 2560–2843) in their study, which does not include the MT-binding region. Deletion of this MT-binding region did not increase MT stability (Zumbunn *et al.*, 2001). Thus, EB1 may promote MT plus-end assembly/disassembly for all interphase MTs (Tirnauer *et al.*, 1999; Rogers *et al.*, 2002), whereas a small fraction in cellular protrusions may be stabilized in growth by an additional decoration of the end with APC. Because Wen *et al.* (2004) showed that APC and EB1 cooperate to cap nocodazole resistant MTs, it is possible that dynamic APC clusters on MT ends can affect dynamic instability independently of EB1, whereas capping requires APC/EB1 cooperation. Interestingly, recently Green *et al.* (2005) showed that EB1 requires an interaction with APC to inhibit pausing MTs in mitosis. Whether this is cell cycle regulated remains to be determined. It is not clear whether APC "selects" certain MTs because of their location in cell protrusions or whether APC selects MTs randomly, and because of their selective stabilization, the APC-decorated MTs end up in or promote the formation of cell protrusions. Alternatively, MTs may select APC that has been deposited at sites in the cellular periphery where protrusive activity is desired. Those MTs

that have been selected may then be stabilized and thus support the formation of the protrusion. How APC is targeted to selected sites in the cell periphery and how possible links between APC and the F-actin cytoskeleton contribute to this process will be important to determine in the future.

ACKNOWLEDGMENTS

We thank Aaron Straight (Stanford University) for the kind advice on protein labeling, Robert A. Weinberg (The Whitehead Institute and Massachusetts Institute for Technology) for mouse primary fibroblasts, Lynn Cassimeris for EB1-pEGFP-N1 construct, R. Agami (The Netherlands Cancer Institute, Amsterdam, The Netherlands) for pSUPER vector, Angela I.M. Barth for anti-EB1 antibodies, Rina Rosin-Arbesfeld and Mariann Bienz (MRC Laboratory of Molecular Biology) for APC-pEGFP-C1 construct, and Hamamatsu Photonics for use of C9100-12 CCD camera. We thank all the members of Waterman-Storer and Näthke laboratories for comments and discussions throughout this work, particularly Mike Adams and Bill Shin for maintenance of microscopes. This study was supported with Uehara Memorial Foundation, Yamanouchi Foundation for Research on Metabolic Disorders, American Heart Association Western States Affiliate Fellowship AHA 0325174Y (to K. K.), Human Frontier Science Program Young Investigator Award Grant RGY5 (to I.S.N., C.M.W.-S., and G. Danuser), and National Institutes of Health Grant GM-61804 to C.M.W.-S. I.S.N. is a Cancer Research UK Senior Research Fellow.

REFERENCES

- Adams, M. C., Matov, A., Yasar, D., Gupton, S. L., Danuser, G., and Waterman-Storer, C. M. (2004). Signal analysis of total internal reflection fluorescent speckle microscopy (TIR-FSM) and wide-field epi-fluorescence FSM of the actin cytoskeleton and focal adhesions in living cells. *J. Microsc.* 216, 138–152.
- Adams, M. C., Salmon, W. C., Gupton, S. L., Cohan, C. S., Wittmann, T., Prigozhina, N., and Waterman-Storer, C. M. (2003). A high-speed multispectral spinning-disk confocal microscope system for fluorescent speckle microscopy of living cells. *Methods* 29, 29–41.
- Akhmanova, A., and Hoogenraad, C. C. (2005). Microtubule plus-end-tracking proteins: mechanisms and functions. *Curr. Opin. Cell Biol.* 17, 47–54.
- Akhmanova, A., *et al.* (2001). CLASPs are CLIP-115 and -170 associating proteins involved in the regional regulation of microtubule dynamics in motile fibroblasts. *Cell* 104, 923–935.
- Allan, V., and Näthke, I. S. (2001). Catch and pull a microtubule: getting a grasp on the cortex. *Nat. Cell Biol.* 3, E226–E228.
- Askham, J. M., Vaughan, K. T., Goodson, H. V., and Morrison, E. E. (2002). Evidence that an interaction between EB1 and p150^{Glued} is required for the formation and maintenance of a radical microtubule array anchored at the centrosome. *Mol. Biol. Cell* 13, 3627–3645.
- Baeg, G.-H., Matsumine, A., Kuroda, T., Bhattacharjee, R. N., Miyashiro, I., Toyoshima, K., and Akiyama, T. (1995). The tumor suppressor gene product APC blocks cell cycle progression from G₀/G₁ to S phase. *EMBO J.* 14, 5618–5625.
- Barth, A.I.M., Siemers, K. A., and Nelson, W. J. (2002). Dissecting interactions between EB1, microtubules and APC in cortical clusters at the plasma membrane. *J. Cell Sci.* 115, 1583–1590.
- Bienz, M. (2002). The subcellular destinations of APC proteins. *Nat. Rev. Mol. Cell Biol.* 3, 328–338.
- Brummelkamp, T. R., Bernards, R., and Agami, R. (2002). A system for stable expression of short interfering RNAs in mammalian cells. *Science* 296, 550–553.
- Carvalho, P., Mohan L. Gupta, J., Hoyt, M. A., and Pellman, D. (2004). Cell cycle control of kinesin-mediated transport of Bik1 (CLIP-170) regulates microtubule stability and dynein activation. *Dev. Cell* 6, 815–829.
- Carvalho, P., Tirnauer, J. S., and Pellman, D. (2003). Surfing on microtubule ends. *Trends Cell Biol.* 13, 229–237.
- Diamantopoulos, G. S., Perez, F., Goodson, H. V., Batelier, G., Melki, R., Kreis, T. E., and Rickard, J. E. (1999). Dynamic localization of CLIP-170 to microtubule plus ends is coupled to microtubule assembly. *J. Cell Biol.* 144, 99–112.
- Dikovskaya, D., Zumbunn, J., Penman, G. A., and Näthke, I. S. (2001). The adenomatous polyposis coli protein: in the limelight out at the edge. *Trends Cell Biol.* 11, 378–384.
- Fodde, R., *et al.* (2001). Mutations in the APC tumor suppressor gene cause chromosomal instability. *Nat. Cell Biol.* 3, 433–438.

- Folker, E. S., Baker, B. M., and Goodson, H. V. (2005). Interactions between CLIP-170, tubulin, and microtubules: implications for the mechanism of CLIP-170 plus-end tracking behavior. *Mol. Biol. Cell* 16, 5373–5384.
- Green, R. A., and Kaplan, K. B. (2003). Chromosome instability in colorectal tumor cells is associated with defects in microtubule plus-end attachments caused by a dominant mutation in APC. *J. Cell Biol.* 163, 949–961.
- Green, R. A., Wollman, R., and Kaplan, K. B. (2005). APC and EB1 function together in mitosis to regulate spindle dynamics and chromosome alignment. *Mol. Biol. Cell* 16, 4609–4622.
- Groden, J., *et al.* (1991). Identification and characterization of the familial adenomatous polyposis coli gene. *Cell* 66, 589–600.
- Gundersen, G. G., Kalnoski, M. H., and Bulinski, J. C. (1984). Distinct populations of microtubules: tyrosinated and nontyrosinated alpha tubulin are distributed differently *in vivo*. *Cell* 38, 779–789.
- Infante, A. S., Stein, M. S., Zhai, Y., Borisy, G. G., and Gundersen, G. G. (2000). Detyrosinated (Glu) microtubules are stabilized by an ATP-sensitive plus-end cap. *J. Cell Sci.* 113, 3907–3919.
- Jimbo, T., Kawasaki, Y., Koyama, R., Sato, R., Takada, S., Haraguchi, K., and Akiyama, T. (2002). Identification of a link between the tumor suppressor APC and the kinesin superfamily. *Nat. Cell Biol.* 4, 323–327.
- Joslyn, G., *et al.* (1991). Identification of deletion mutations and three new genes at the familial polyposis locus. *Cell* 66, 601–613.
- Kaplan, K. B., Burds, A. A., Swedlow, J. R., Bekir, S. S., Sorger, P. K., and Näthke, I. S. (2001). A role for the adenomatous polyposis coli protein in chromosome segregation. *Nat. Cell Biol.* 3, 429–432.
- Kawasaki, Y., Sato, R., and Akiyama, T. (2003). Mutated APC and Asef are involved in the migration of colorectal tumor cells. *Nat. Cell Biol.* 5, 211–215.
- Kawasaki, Y., Senda, T., Ishidate, T., Koyama, R., Morishita, T., Iwayama, Y., Higuchi, O., and Akiyama, T. (2000). Asef, a link between the tumor suppressor APC and G-protein signaling. *Science* 289, 1194–1197.
- Kirschner, M., and Mitchison, T. (1986). Beyond self-assembly: from microtubules to morphogenesis. *Cell* 45, 329–342.
- Komarova, Y. A., Akhmanova, A. S., Kojima, S.-I., Galjart, N., and Borisy, G. G. (2002). Cytoplasmic linker proteins promote microtubule rescue *in vivo*. *J. Cell Biol.* 159, 589–599.
- Li, Z., and Näthke, I. S. (2005). Tumor-associated NH₂-terminal fragments are the most stable part of the adenomatous polyposis coli protein and can be regulated by interactions with COOH-terminal domains. *Cancer Res.* 65, 5195–5204.
- Liao, G., Nagasaki, T., and Gundersen, G. G. (1995). Low concentrations of nocodazole interfere with fibroblast locomotion without significantly affecting microtubule level: implications for the role of dynamic microtubules in cell locomotion. *J. Cell Sci.* 108, 3473–3483.
- Ligon, L. A., Shelly, S. S., Tokito, M., and Holzbaur, E.L.F. (2003). The microtubule plus-end proteins EB1 and dynactin have differential effects on microtubule polymerization. *Mol. Biol. Cell* 14, 1405–1417.
- Louie, R. K., Bahmanyar, S., Siemers, K. A., Votin, V., Chang, P., Stearns, T., Nelson, W. J., and Barth, A.I.M. (2004). Adenomatous polyposis coli and EB1 localize in close proximity of the mother centriole and EB1 is a functional component of centrosomes. *J. Cell Sci.* 117, 1117–1128.
- Maddox, P., Straight, A., Coughlin, P., Mitchison, T. J., and Salmon, E. D. (2003). Direct observation of microtubule dynamics at kinetochores in *Xenopus* extract spindles: implications for spindle mechanics. *J. Cell Biol.* 162, 377–382.
- Mahmoud, N. N., Boolbol, S. K., Bilinski, R. T., Martucci, C., Chadburn, A., and Bertagnolli, M. M. (1997). *Apc* gene mutation is associated with a dominant-negative effect upon intestinal cell migration. *Cancer Res.* 57, 5045–5050.
- Matsumine, A., *et al.* (1996). Binding of APC to the human homolog of the *Drosophila* discs large tumor suppressor protein. *Science* 272, 1020–1023.
- Mimori-Kiyosue, Y., *et al.* (2005). CLASP1 and CLASP2 bind to EB1 and regulate microtubule plus-end dynamics at the cell cortex. *J. Cell Biol.* 168, 141–153.
- Mimori-Kiyosue, Y., Shiina, N., and Tsukita, S. (2000a). Adenomatous polyposis coli (APC) protein moves along microtubules and concentrates at their growing ends in epithelial cells. *J. Cell Biol.* 148, 505–517.
- Mimori-Kiyosue, Y., Shiina, N., and Tsukita, S. (2000b). The dynamic behavior of the APC-binding protein EB1 on the distal ends of microtubules. *Curr. Biol.* 10, 865–868.
- Mimori-Kiyosue, Y., and Tsukita, S. (2003). “Search-and-capture” of microtubules through plus-end-binding proteins (+TIPs). *J. Biochem.* 134, 321–326.
- Mimori-Kiyosue, Y., and Tsukita, S. (2001). Where is APC going? *J. Cell Biol.* 154, 1105–1109.
- Morin, P. J., Vogelstein, B., and Kinzler, K. W. (1996). Apoptosis and APC in colorectal tumorigenesis. *Proc. Natl. Acad. Sci. USA* 93, 7950–7954.
- Morrison, E. E., Wardleworth, B. N., Askham, J. M., Markham, A. F., and Meredith, D. M. (1998). EB1, a protein which interacts with the APC tumor suppressor, is associated with the microtubule cytoskeleton throughout the cell cycle. *Oncogene* 17, 3471–3477.
- Munemitsu, S., Albert, I., Souza, B., Rubinfeld, B., and Polakis, P. (1995). Regulation of intracellular β -catenin levels by the adenomatous polyposis coli (APC) tumor-suppressor protein. *Proc. Natl. Acad. Sci. USA* 92, 3046–3050.
- Munemitsu, S., Souza, B., Müller, O., Albert, I., Rubinfeld, B., and Polakis, P. (1994). The APC gene product associates with microtubules *in vivo* and promotes their assembly *in vitro*. *Cancer Res.* 54, 3676–3681.
- Nakamura, M., Zhou, X. Z., and Lu, K. P. (2001). Critical role for the EB1 and APC interaction in the regulation of microtubule polymerization. *Curr. Biol.* 11, 1062–1067.
- Näthke, I. S. (2004). The adenomatous polyposis coli protein: the Achilles heel of the gut epithelium. *Annu. Rev. Cell Dev. Biol.* 20, 337–366.
- Näthke, I. S., Adams, C. L., Polakis, P., Sellin, J. H., and Nelson, W. J. (1996). The adenomatous polyposis coli tumor suppressor protein localizes to plasma membrane sites involved in active cell migration. *J. Cell Biol.* 134, 165–179.
- Piehl, M., and Cassimeris, L. (2003). Organization and dynamics of growing microtubule plus ends during early mitosis. *Mol. Biol. Cell* 14, 916–925.
- Polakis, P. (2000). Wnt signaling and cancer. *Genes Dev.* 14, 1837–1851.
- Reilein, A., and Nelson, W. J. (2005). APC is a component of an organizing template for cortical microtubule networks. *Nat. Cell Biol.* 7, 463–473.
- Riess, N. P., Milward, K., Lee, T., Adams, M., Askham, J. M., and Morrison, E. E. (2005). Trapping of normal EB1 ligands in aggresomes formed by an EB1 deletion mutant. *BMC Cell Biol.* 6, 17.
- Rogers, S. L., Rogers, G. C., Sharp, D. J., and Vale, R. D. (2002). *Drosophila* EB1 is important for proper assembly, dynamics, and positioning of the mitotic spindle. *J. Cell Biol.* 158, 873–884.
- Rosin-Arbesfeld, R., Ihrke, G., and Bienz, M. (2001). Actin-dependent membrane association of the APC tumor suppressor in polarized mammalian epithelial cells. *EMBO J.* 20, 5929–5939.
- Rubinfeld, B., Souza, B., Albert, I., Müller, O., Chamberlain, S. H., Masiarz, F. R., Munemitsu, S., and Polakis, P. (1993). Association of the APC gene product with β -catenin. *Science* 262, 1731–1734.
- Sansom, O. J., *et al.* (2004). Loss of Apc *in vivo* immediately perturbs Wnt signaling, differentiation, and migration. *Genes Dev.* 18, 1385–1390.
- Smith, K. J., Levy, D. B., Maupin, P., Pollard, T. D., Vogelstein, B., and Kinzler, K. W. (1994). Wild-type but not mutant APC associates with the microtubule cytoskeleton. *Cancer Res.* 54, 3672–3675.
- Su, L.-K., Burrell, M., Hill, D. E., Gyuris, J., Brent, R., Wiltshire, R., Trent, J., Vogelstein, B., and Kinzler, K. W. (1995). APC binds to the novel protein EB1. *Cancer Res.* 55, 2972–2977.
- Su, L.-K., Vogelstein, B., and Kinzler, K. W. (1993). Association of the APC tumor suppressor protein with catenins. *Science* 262, 1734–1737.
- Tirnauer, J. S., Grego, S., Salmon, E. D., and Mitchison, T. J. (2002). EB1-microtubule interactions in *Xenopus* egg extracts: role of EB1 in microtubule stabilization and mechanisms of targeting to microtubules. *Mol. Biol. Cell* 13, 3614–3626.
- Tirnauer, J. S., O’Toole, E., Berrueta, L., Bierer, B. E., and Pellman, D. (1999). Yeast Bim1p promotes the G1-specific dynamics of microtubules. *J. Cell Biol.* 145, 993–1007.
- Wadsworth, P. (1999). Regional regulation of microtubule dynamics in polarized, motile cells. *Cell Motil. Cytoskeleton* 42, 48–59.
- Watanabe, T., *et al.* (2004). Interaction with IQGAP1 links APC to Rac1, Cdc42, and actin filaments during cell polarization and migration. *Dev. Cell* 7, 871–883.
- Waterman-Storer, C. M. (2002). Fluorescent speckle microscopy (FSM) of microtubules and actin in living cells. In: *Current Protocols in Cell Biology*, Vol. 1, ed. J. S. Bonifacino, M. Dasso, J. B. Harford, J. Lippincott-Schwartz, and K. M. Yamada, New York: John Wiley & Sons, 4.10.1–4.10.26.
- Waterman-Storer, C. M., and Salmon, E. D. (1997). Actomyosin-based retrograde flow of microtubules in the lamella of migrating epithelial cells influences microtubule dynamic instability and turnover and is associated with microtubule breakage and treadmill. *J. Cell Biol.* 139, 417–434.
- Wen, Y., Eng, C. H., Schmoranzler, J., Cabrera-Poch, N., Morris, E.J.S., Chen, M., Wallar, B. J., Alberts, A. S., and Gundersen, G. G. (2004). EB1 and APC

- bind to mDia to stabilize microtubules downstream of Rho and promote cell migration. *Nat. Cell Biol.* 6, 820–830.
- Wittmann, T., Bokoch, G. M., and Waterman-Storer, C. M. (2003). Regulation of leading edge microtubule and actin dynamics downstream of Rac1. *J. Cell Biol.* 161, 845–851.
- Wittmann, T., Bokoch, G. M., and Waterman-Storer, C. M. (2004). Regulation of microtubule destabilizing activity of Op18/stathmin downstream of Rac1. *J. Biol. Chem.* 279, 6196–6203.
- Wittmann, T., and Waterman-Storer, C. M. (2005). Spatial regulation of CLASP affinity for microtubules by Rac1 and GSK3 β in migrating epithelial cells. *J. Cell Biol.* 169, 929–939.
- Wong, M. H., Hermiston, M. L., Syder, A. J., and Gordon, J. I. (1996). Forced expression of the tumor suppressor adenomatosis polyposis coli protein induces disordered cell migration in the intestinal epithelium. *Proc. Natl. Acad. Sci. USA* 93, 9588–9593.
- Yu, X., Waltzer, L., and Bienz, M. (1999). A new *Drosophila* APC homologue associated with adhesive zones of epithelial cells. *Nat. Cell Biol.* 1, 144–151.
- Zumbrunn, J., Kinoshita, K., Hyman, A. A., and Nathke, I. S. (2001). Binding of the adenomatous polyposis coli protein to microtubules increases microtubule stability and is regulated by GSK3 β phosphorylation. *Curr. Biol.* 11, 44–49.